COMMUNICATION

Radical Chemistry and Reaction Mechanisms of Propane Oxidative Dehydrogenation over Hexagonal Boron Nitride Catalysts

Xuanyu Zhang[+], Rui You[+], Zeyue Wei, Xiao Jiang, Jiuzhong Yang, Yang Pan, Peiwen Wu, Qingdong Jia, Zhenghong Bao, Lei Bai, Mingzhou Jin, Bobby Sumpter, Victor Fung*, Weixin Huang* and Zili Wu *

Abstract: Although hexagonal boron nitride (h-BN) has recently been identified as a highly efficient catalyst for the oxidative dehydrogenation of propane (ODHP) reaction, the reaction mechanisms, especially regarding radical chemistry of this system, remain elusive. Herein we report the first direct experimental evidence of gas-phase methyl radicals (CH_3·) in the ODHP reaction over boron-based catalysts by using an online synchrotron vacuum ultraviolet photoionization mass spectroscopy (SVUV-PIMS), which uncovers the existence of gas-phase radical pathways. Combined with density functional theory (DFT) calculations, our results demonstrate that propene is mainly generated on the catalyst surface from the C-H activation of propane while C_2 and C_1 products can be formed via both surface-mediated and gas-phase pathways. These observations provide new insights towards understanding the ODHP reaction mechanisms over boron-based catalysts.

Propene (C_3H_6) is mainly produced by the steam cracking of oil-derived naphtha or the direct dehydrogenation of propane (PDH).[1] As a promising alternative, the oxidative dehydrogenation of propane (ODHP), has gathered significant attention due to its thermodynamic favorability characterized by low reaction temperatures and suppression of coking.[2] However, the commercialization of the ODHP process has not been achieved because of the runaway over-oxidation of olefins leading to significant amounts of CO_x. Recently, several research groups have reported that hexagonal boron nitride (h-BN) is an outstanding and selective catalyst for the ODH of alkanes to corresponding olefins with only negligible CO_x formation.[3] It is generally proposed that the formed oxidized B sites (e.g., B-O, B-OH and $B(OH)_xO_{3-x}$) act as the active centers under ODHP reaction conditions.[4] Different from the traditional vanadium and molybdenum-based redox metal oxide catalysts in ODHP reaction, h-BN shows very low selectivity to carbon oxides and relatively high selectivity to ethylene, compared to V-based catalysts where the main by-products are CO_x.[5] The drastically different product distributions observed in the h-BN and metal oxide-based catalysts imply that the reaction mechanisms are different in these two types of catalysts. Generally, the ODHP reaction catalyzed by transition metal oxide catalysts was demonstrated to follow the redox mechanism, in which the oxidation of propane by surface lattice oxygen of transitional metal oxides is the rate-limiting step.[1a,5a,5c]

Interestingly, a recent work implied a possible influence of gas-phase radical chemistry of h-BN catalyst in ODHP reaction,[6] in which no expected relationship was found between the catalytic activity and contact time. Wang et.al.[7] have proposed that methyl radicals are generated on the h-BN surface from the C-C bond cleavage, leading to various secondary reaction pathways involving methyl radicals during ODHP. However, to date there is no direct experimental evidence for the presence of radicals in the ODHP reaction over h-BN catalyst, possibly due to the high reactivity and short lifetime of the gas-phase radicals. In this regard, synchrotron radiation vacuum ultraviolet photoionization mass spectroscopy (SVUV-PIMS) is an emerging powerful tool for direct online detection of reactive, unstable, and short-lived gas-phase radicals and intermediates for various heterogeneous catalytic reactions.[8] Herein, we report *for the first time* that gas-phase methyl radicals (CH_3·) can be directly observed in the ODHP reaction over h-BN and suppoted boron oxide catalysts. Furthermore, the complete reaction pathways and mechanisms of ODHP reaction over the h-BN catalysts are proposed with the aid of combined kinetic study, SVUV-PIMS measurement, and density functional theory (DFT) calculations.

A high BET surface area h-BN catalyst (72.7 $m^2 g^{-1}$), denoted as BN-high, was prepared via a novel gas exfoliation of bulk h-BN in liquid N_2.[9] The commercial h-BN catalyst (BN-low) was purchased from Johnson Matthey INC. with a low BET surface area (3.7 $m^2 g^{-1}$). Before ODHP tests, all the h-BN catalysts were treated by reaction feed gas (C_3H_8:O_2:He = 1:1:38, total flow rate

[*] X, Zhang,[+] R, You,[+] Z, Wei, W. Huang
Hefei National Laboratory for Physical Sciences at the Microscale, Key Laboratory of Surface and Interface Chemistry and Energy Catalysis of Anhui Higher Education Institutes, CAS key Laboratory of Materials for Energy Conversion and Department of Chemical Physics, University of Science and Technology of China
Heifei 230026 (P. R. China)
E-mail: huangwx@ustc.edu.cn
X, Zhang,[+] X, Jiang, Z, Bao, L, Bai, Z, Wu
Chemical Sciences Division and Center for Nanophase Materials Science, Oak Ridge National Laboratory
Oak Ridge, TN 37831 (USA)
E-mail: wuz1@ornl.gov
B, Sumpter, V, Fung.
Center for Nanophase Materials Science and Computational Sciences & Engineering Division, Oak Ridge National Laboratory
Oak Ridge, TN 37831 (USA)
E-mail: fungv@ornl.gov
J, Yang, Y, Pan
National Synchrotron Radiation Laboratory, University of Science and Technology of China
Heifei 230026 (P. R. China)
P, Wu, Q, Jia
School of Chemistry and Chemical Engineering, Jiang Su University
Zhenjiang 212013 (P.R. China)
M, Jin
Institute of a Secure and Sustainable Environment
The University of Tennessee, Knoxville
Knoxville, TN 37996 (USA)
[+] These authors contributed equally to this work.

Supporting information for this article is given via a link at the end of the document.

30 mL min^{-1}) at 500 °C for 12 h (denoted as BN-T). There was a negligible change of BET surface area after the ODHP reaction condition treatment (See Table S1). The X-ray diffraction (XRD) patterns only showed peaks arising from the hexagonal boron nitride in fresh and treated catalysts (Figure S1A). Raman spectra of these samples exhibited a strong B-N E_{2g} mode around 1370 cm^{-1} (Figure S1B) with no obvious change before and after the treatment.[10] The E_{2g} mode was broader for the BN-high catalysts, due to the smaller crystal grain size[10b] than the BN-low samples. The morphology of the fresh and treated h-BN catalysts showed no significant changes from scanning electron microscopy (Figure S2). The XRD, Raman and SEM results indicate no evident changes to the bulk structure and physical property of BN after the treatment.

The chemical structure was further characterized with FTIR spectroscopy (Figure S3) and XPS (Figures S4 and S5). The IR band at around 1325 cm^{-1} can be assigned to the in-plane B-N Transverse Optical (TO) modes of h-BN, while the band at 815 cm^{-1} corresponded to the out-of-plane B-N-B bending vibration.[3d,11] A new IR peak at 690 cm^{-1} and a broad one at 3200 cm^{-1} appeared on the treated h-BN samples, and were attributed to the O-B-O and B-OH modes, respectively.[3e,11b] Further, the B 1s XPS spectra of treated BN samples (Figure S4 and S5) exhibited major peaks at 190.6 and 192.2 eV, corresponding to B-N and B-O bonds, respectively.[3d,4a,11b,11d] The proportion of B-O bonds was calculated from the B 1s spectra, and the ratio of O/B increased when BN was treated in ODHP reaction atmosphere at 500 °C (Table S1), which indicates the increment of B-OH and B-O species.[11c] The results from FTIR and XPS agree well with previous studies, showing that the BN surface is oxidized and hydrolyzed to form B-O and B-OH species under ODH reaction conditions.[4c,4f,11b]

The temperature-dependent catalytic performance of the ODHP reaction over the various treated h-BN and BO_x/SiO_2 catalysts is shown in Figure 1 and Figure S6, respectively. On the BN-T-high sample, the reaction started from the temperature of 500 °C with a low propane conversion of 0.3% and reached the highest conversion (38.2%) at 600 °C. Compared with the activity of BN-T-low sample (Figure S6A), the propane conversion is almost four times higher over the BN-T-high catalyst with comparable olefin selectivity, owing to a relatively low BET surface area and fewer surface B-O and B-OH sites on the BN-T-low sample. The stability test was evaluated for BN-T-high catalyst at 600 °C for 24 hours and the conversion of propane is stable at ~43% with selectivity remained at around 75% for C_2+C_3 alkenes (Figure S7). A re-run of the 600 °C-tested BN-high sample showed similar catalytic performance (Figure S7) to the 500 °C-treated one (Figure 1), indicating similar surface sites on BN after the two temperature treatments.

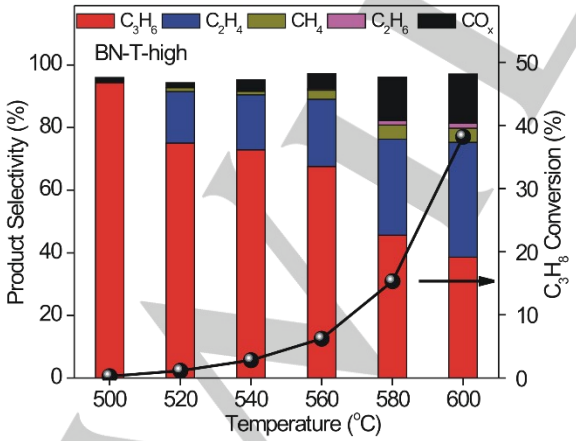

Figure 1. Influence of temperature on the catalytic performance of ODHP reaction over BN-T-high catalyst. Reaction condition: 100 mg of catalyst; gas feed, 2.5 vol% C_3H_8, 2.5 vol% O_2, He balance; flow rate 30 mL min^{-1}.

The product distributions of BN catalysts were quite different from the traditional metal oxide catalysts, where the main by-product is C_2H_4, and its selectivity increased with C_3H_8 conversion especially at high temperatures. As shown in Figure S6B, the BOx/SiO_2 catalyst showed similar product distributions in the ODHP reaction as on the BN samples. This similarity suggests similar surface sites for ODHP over the two type of catalysts. We detected traces of nitric oxide (NO) on BN-T-high catalyst at high temperatures at high propane conversion (Figure S8). The catalytic conversion of ODHP over both BN-T-high and BN-T-low did not change linearly with the different gas space velocities (Figure S9). The absence of mass and heat transfer limitation in the ODHP tests was verified by Weisz-Prater analysis and Mears analysis, respectively (see SI for detailed calculation). Meanwhile, the high E_a values (>170 kJ/mol) over the different boron-based catlaysts were addtional evidence for the absence of diffusion limitation (Figure S10). This observation is consistent with previous research.[6] Specifically, the gas-phase radicals [6-7] were proposed as the key reaction intermediates in ODHP reaction over BN catalysts, however the direct experimental evidence for the gas-phase radicals is still lacking.

To investigate the possible radical chemistry, the gas-phase components of the ODHP reaction over h-BN-T catalysts were analyzed online by synchrotron radiation vacuum ultraviolet photoionization mass spectroscopy (SVUV-PIMS) (Figure S11-S18, and see the SI for the detailed gas-phase components analysis). Figure 2A shows the SVUV-PIMS spectrum of gas-phase intermediates catalyzed by BN-T-high during ODHP reaction at 600 °C ionized at a photon energy of 10.0 eV. The obvious signals at m/z values of 15.03 and 42.08 were assigned to methyl radicals (CH_3·) and propene (C_3H_6), respectively, with reference to online standard database[12] and our previous work.[8d-f] In addition, we also detected the methyl radicals (CH_3·) in BN-T-low and BO_x/SiO_2 catalysts (Figure S11, S15, and S19). The control and blank tests (Figure S20) showed no evident gas-phase methyl radicals signal (m/z=15) with the presence of catalyst at room temperature and without catalyst at 600 °C, implying that all detected gas-phase methyl radicals should be produced from the activation of propane on the catalyst surface during ODHP reactions. Furthermore, the generation of methyl radicals was observed throughout the ODHP reaction even at low temperatures with low C_3H_8 conversions over the h-BN and BO_x/SiO_2 catalysts (Figure S21). This suggests that the working BN catalysts and the BO_x/SiO_2 indeed may have similar surface active sites for the ODHP reaction. Our SVUV-PIMS results provided direct and unambiguous detection of gas-phase methyl radicals in the ODHP reaction catalyzed by h-BN and BO_x/SiO_2 catalysts. To our knowledge, this is *the first report* of direct experimental evidence of methyl radical generation in ODHP reaction over boron-based catalysts. Meanwhile, any gas-phase ethyl (C_2H_5·) and propyl (C_3H_7·) radicals were not detected in this system. In our recent work, we have successfully detected propyl radicals by the same SVUV-PIMS with high sensitivity and

mass resolution in ODHP reaction, even at very low concentration of gas-phase radicals.[8e] Combined with this experimental phenomenon, we can speculate that propyl radicals are not formed, or the contribution is very limit in this reaction system.

The integrated peak intensity of signals of various gas-phase components in the SVUV-PIMS spectra of the ODHP reaction catalyzed by BN-T-high sample was plotted as a function of temperature and shown in Figure 2B. With the increasing of reaction temperature from 500 to 600 °C, there was an obvious growth of the signals for C_2H_4, C_2H_6, and HCHO, whereas the integrated ion intensities of CH_3·, CH_4, and CO_x increased slowly with the reaction temperature. This similar growth trend of integrated ion intensities suggests that some of C_1 and C_2 products should be formed by the secondary gas-phase reaction of surface-generated methyl radicals. [7,8f] Meanwhile, the main product, propene, is more likely formed on the catalyst surface, since no gas-phase propyl radicals were observed.

Noteworthily, we detected NO on BN-T-high catalyst during ODHP reaction at 600 °C by using the SVUV-PIMS (Figure S22), which was consistent with the GC-TCD results (Figure S8). The presence of NO may also affect the formation of gas-phase radicals in the alkane reaction system as demonstrated recently in catalyst-free propane ODH in empty reactors in the presence of O_2 at around 500 °C.[14] Therefore, the effect of NO on ODHP reaction over the BN catalysts warrants more attention, and further investigation is currently ongoing in our lab. However, the detection of methyl radical over BOx/SiO_2 (Figure S21) in the absence of NO suggests that radical chemistry over boron-based catalysts for ODHP reaction is indeed present regardless of NO presence.

DFT calculations were performed to construct the reaction mechanism including pathways and radical chemistry of ODHP on the boron nitride catalyst. Based on our experimental characterizations (IR and XPS) and previous studies of boron nitride catalysts under ODHP reaction conditions, the active phase of the catalyst can be characterized as an amporphous boron oxide layer with $B(OH)_xO_{3-x}$ sites.[4f] In our DFT study, a surface model was constructed from B_2O_3 containing surface BO_3 units (Figure S23, further discussion of surface model in SI).

As shown in Figure 3, the first step in ODHP is the C-H activation of propane, which we find to most likely occur via a heterolytic cleavage over a B-O pair in a BO_3 active site (Figure S28). This step occurs with a barrier of 1.73 eV to form a co-adsorbed B-C_3H_7 on the boron and a hydrogen on the B-O-B oxygen (steps A-C in Figure 3). To drive the formation of propene from propyl on the surface, O_2 is required by first abstracting the hydrogen from the surface O-H with a barrier of 0.73 eV (steps D-F in Figure 3), which reduces the O_2 to HO_2. This process results in a weakly bound B-HO_2 and B-C_3H_7 on adjacent BO_3 sites. This is followed by a reaction of the two surface species by HO_2 abstracting the hydrogen from the propyl to form H_2O_2 (steps F-G in Figure 3), a thermodynamically downhill step which can occur with little to no energy barrier. Both propene and H_2O_2 then desorb readily from the surface and H_2O_2 decomposes to form water, closing the cycle and regenerating the BO_3 site. We have also explored the formation of C_1 and C_2 products which start to form in larger proportions at higher temperatures (Figure 1). We find the formation of such as ethylene and methyl radicals can occur competitively over either the surface or the gas-phase (Figures S30, 31) with similar barriers.

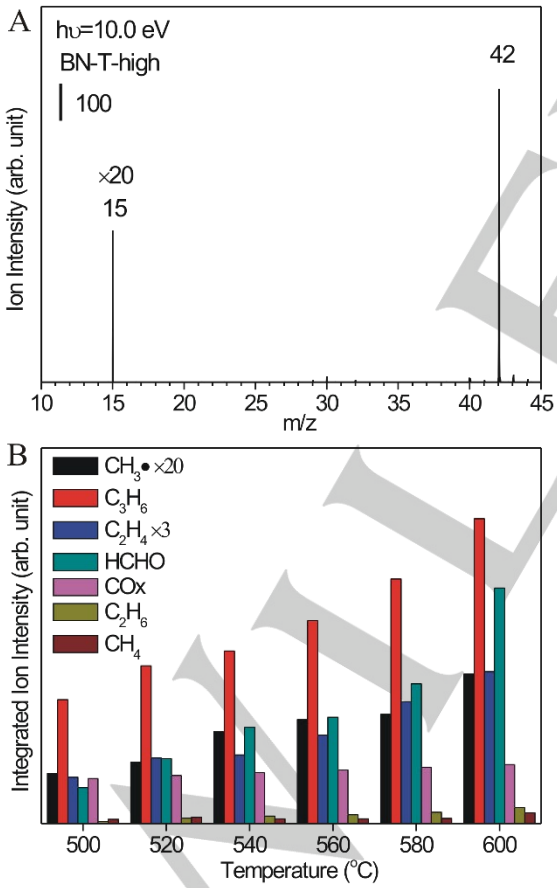

Figure 2. (A) SVUV-PIMS spectra of gas-phase components of the ODHP reaction catalyzed by BN-T-high at 600 °C acquired with a photon energy of 10.0 eV. (B) Integrated ion intensities of various components detected during the ODHP reaction catalyzed by BN-T-high at different temperatures.

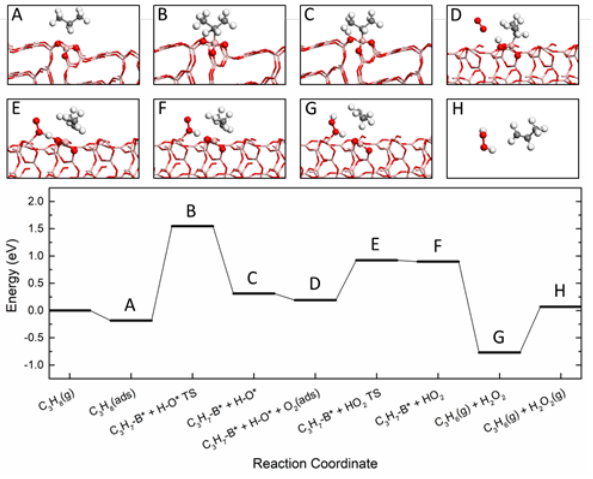

Figure 3. DFT calculated energy profile for propane oxidative hydrogenation to propene over B-O-B site on B_2O_3(101) surface. From left to right, the initial state, transition state and final states are shown. The models A – H show the side-view of the geometries of varies steps. The BO_3 active site is highlighted with ball-and-stick models.

In the absence of an oxidant such as O_2, the C_3H_7 intermediate is inert to surface-mediated C-H activation and further oxidation (Figure S32), though gas-phase unimolecular cleavage could still occur. The high thermodynamic (and kinetic) unfavorability of the subsequent C-H activation by the B-O-B oxygen is explained by poor redox ability of the surface, which differs from conventional ODHP catalysts such as vanadia and other transition metal oxides.[16] Instead, we have found the redox-poor surface catalyzes the reaction by heterolytic C-H cleavage followed by a reduction of the gas phase oxidant rather than the surface. The proposed mechanism bears similarities to other redox-poor oxides such as MgO,[17] and shares their capacity for selective alkane conversions.

In summary, we have successfully demonstrated that the ODHP reaction catalyzed by both h-BN and suppored boron oxide catalysts involves the gas-phase radical mechanisms and pathways with unambiguously identified gas-phase methyl radicals by using the SVUV-PIMS. By coupling the results from kinetic and SVUV-PIMS studies with DFT calculations, detailed reaction pathways are proposed for the various products from ODHP over boron-based catalysts. Propene is mainly formed from surface reaction via the cleavage of C-H bonds of propane. Both surface-mediated and gas-phase reactions pathways can contribute to the C_1 and C_2 products. Our findings provide new insights towards understanding the ODHP reaction mechanisms and pathways over boron-based catalysts and are of significance for developing highly selective catalysts for alkane ODH.

Acknowledgements

This work was supported by the Center for Understanding and Control of Acid Gas-Induced Evolution of Materials for Energy (UNCAGE-ME), an Energy Frontier Research Center funded by U.S. Department of Energy, Office of Science, Basic Energy Sciences. X.Z, R.Y, Z.Y.W and W.H were supported by the National Natural Science Foundation of China (21525313, 91745202, 21703227), the Chinese Academy of Sciences, the Changjiang Scholars Program of Ministry of Education of China, and the China Scholarship Council. Part of the work incluidng the synthesis and catalysis test was done at the Center for Nanophase Materials Sciences, which is a DOE Office of Science User Facility.

Keywords: hexagonal boron nitride • oxidative dehydrogenation • mass spectroscopy • methyl radical • reaction pathway

[1] a) J. J. Sattler, J. Ruiz-Martinez, E. Santillan-Jimenez, B. M. Weckhuysen, *Chem. Rev.* **2014**, *114*, 10613-10653; b) L. Zhong, F. Yu, Y. An, Y. Zhao, Y. Sun, Z. Li, T. Lin, Y. Lin, X. Qi, Y. Dai, L. Gu, J. Hu, S. Jin, Q. Shen, H. Wang, *Nature* **2016**, *538*, 84-87.

[2] E. G. Rightor, C. L. Tway, *Catal. Today* **2015**, *258*, 226-229.

[3] a) J. T. Grant, C. A. Carrero, F. Goeltl, J. Venegas, P. Mueller, S. P. Burt, S. E. Specht, W. P. McDermott, A. Chieregato, I. Hermans, *Science* **2016**, *354*, 1570-1573; b) J. M. Venegas, W. P. McDermott, I. Hermans, *Acc. Chem. Res.* **2018**, *51*, 2556-2564; c) L. Shi, Y. Wang, B. Yan, W. Song, D. Shao, A. H. Lu, *Chem. Commun.* **2018**, *54*, 10936-10946; d) F. Guo, P. Yang, Z. Pan, X. N. Cao, Z. Xie, X. Wang, *Angew. Chem. Int. Ed.* **2017**, *56*, 8231-8235; e) L. Shi, D. Q. Wang, A. H. Lu, *Chin. J. Catal.* **2018**, *39*, 908-913; f) P. Chaturbedy, M. Ahamed, M. Eswaramoorthy, *ACS Omega* **2018**, *3*, 369-374.

[4] a) L. Shi, D. Q. Wang, W. Song, D. Shao, W. P. Zhang, A. H. Lu, *ChemCatChem* **2017**, *9*, 1788-1793; b) L. Shi, B. Yan, D. Shao, F. Jiang, D. Q. Wang, A. H. Lu, *Chin. J. Catal.* **2017**, *38*, 389-395; c) B. Yan, W. C. Li, A. H. Lu, *J. Catal.* **2019**, *369*, 296-301; d) R. Huang, B. S. Zhang, J. Wang, K. H. Wu, W. Shi, Y. J. Zhang, Y. F. Liu, A. M. Zheng, R. Schlögl, D. S. Su, *ChemCatChem* **2017**, *9*, 3293-3297; e) J. T. Grant, W. P. McDermott, J. M. Venegas, S. P. Burt, J. Micka, S. P. Phivilay, C. A. Carrero, I. Hermans, *ChemCatChem* **2017**, *9*, 3623-3626; f) A. M. Love, B. Thomas, S. E. Specht, M. P. Hanrahan, J. M. Venegas, S. P. Burt, J. T. Grant, M. C. Cendejas, W. P. McDermott, A. J. Rossini, I. Hermans, *J. Am. Chem. Soc.* **2019**, *141*, 182-190; g) N. Altvater, R. Dorn, M. Cendejas, W. McDermott, B. Thomas, A. Rossini, I. Hermans, *Angew. Chem. Int. Ed.* 10.1002/anie.201914696; h) W.-D. Lu, D. Wang, Z. Zhao, W. Song, W.-C. Li, A.-H. Lu, *ACS Catal.* **2019**, 8263-8270.

[5] a) C. A. Carrero, R. Schloegl, I. E. Wachs, R. Schomaecker, *ACS Catal.* **2014**, *4*, 3357-3380; b) F. Cavani, N. Ballarini, A. Cericola, *Catal. Today* **2007**, *127*, 113-131; c) S. Barman, N. Maity, K. Bhatte, S. Ould-Chikh, O. Dachwald, C. Haeßner, Y. Saih, E. Abou-Hamad, I. Llorens, J.-L. Hazemann, K. Köhler, V. D' Elia, J.-M. Basset, *ACS Catal.* **2016**, *6*, 5908-5921.

[6] J. M. Venegas, I. Hermans, *Org. Process Res. Dev.* **2018**, *22*, 1644-1652.

[7] J. S. Tian, J. Q. Tan, M. L. Xu, Z. X. Zhang, S. L. Wan, S. Wang, J. D. Lin, Y. Wang, *Sci. Adv.* **2019**, *5*, eaav8063.

[8] a) K. Kohse-Hoinghaus, P. Osswald, T. A. Cool, T. Kasper, N. Hansen, F. Qi, C. K. Westbrook, P. R. Westmoreland, *Angew. Chem. Int. Ed.* **2010**, *49*, 3572-3297; b) F. Battin-Leclerc, O. Herbinet, P. A. Glaude, R. Fournet, Z. Zhou, L. Deng, H. Guo, M. Xie, F. Qi, *Angew. Chem. Int. Ed.* **2010**, *49*, 3169-3172; c) Y. Li, F. Qi, *Acc. Chem. Res* **2010**, *43*, 68-78; d) L. F. Luo, X. F. Tang, W. D. Wang, Y. Wang, S. B. Sun, F. Qi, W. X. Huang, *Sci. Rep.* **2013**, *3*, 1625-1632; e) R. You, X. Y. Zhang, L. F. Luo, Y. Pan, H. B. Pan, J. Z. Yang, L. H. Wu, X. S. Zheng, Y. K. Jin, W. X. Huang, *J. Catal.* **2017**, *348*, 189-199; f) L. F. Luo, R. You, Y. M. Liu, J. Z. Yang, Y. N. Zhu, W. Wen, Y. Pan, F. Qi, W. X. Huang, *ACS Catal.* **2019**, *9*, 2514-2520; g) F. Jiao, J. J. Li, X. L. Pan, J. P. Xiao, H. B. Li, H. Ma, M. M. Wei, Y. Pan, Z. Y. Zhou, M. R. Li, S. Miao, J. Li, Y. F. Zhu, D. Xiao, T. He, J. Yang, F. Qi, X. H. Bao, *Science* **2016**, *351*, 1065-1068; h) R. You, W. X. Huang, *ChemCatChem* **2020,** 12, 675-688.

[9] W. Zhu, X. Gao, Q. Li, H. Li, Y. Chao, M. Li, S. M. Mahurin, H. Li, H. Zhu, S. Dai, *Angew. Chem. Int. Ed.* **2016**, *55*, 10766-10770.

[10] a) J. Wu, W.-Q. Han, W. Walukiewicz, J. Ager, W. Shan, E. Haller, A. Zettl, *Nano Lett.* **2004**, *4*, 647-650; b) R. Arenal, A. Ferrari, S. Reich, L. Wirtz, J.-Y. Mevellec, S. Lefrant, A. Rubio, A. Loiseau, *Nano Lett.* **2006**, *6*, 1812-1816.

[11] a) J. A. Loiland, Z. Zhao, A. Patel, P. Hazin, *Ind. Eng. Chem. Res.* **2019**, *58*, 2170-2180; b) Y. L. Zhou, J. Lin, L. Li, X. L. Pan, X. C. Sun, X. D. Wang, *J. Catal.* **2018**, *365*, 14-23; c) S. Namba, A. Takagaki, K. Jimura, S. Hayashi, R. Kikuchi, S. Ted Oyama, *Catal. Sci. Technol.* **2019**, *9*, 302-309; d) J. H. Wu, L. C. Wang, X. Yang, B. L. Lv, J. Chen, *Ind. Eng. Chem. Res.* **2018**, *57*, 2805-2810.

[12] P.J. Linstrom, W.G. Mallard, NIST Chemistry Webbook, National Institute of Standards and Technology, Gaithersburg, MD, 2008, Number, <http://webbook.nist.gov.chemistry>.

[13] Internet Bond-energy Databank (pKa and BDE)-iBonD, http://ibond.nankai.edu.cn/.

[14] a) L. Annamalai, Y. Liu, P. Deshlahra, *ACS Catal.* **2019**, *9*, 10324-10338; b) J. M. Zalc, W. H. Green, E. Iglesia, *Ind. Eng. Chem. Res.* **2006**, *45*,

2677-2688; c) K. Tabata, Y. Teng, T. Takemoto, E. Suzuki, M. A. Bañares, M. A. Peña, J. L. G. Fierro, *Catal. Rev.* **2002**, *44*, 1-58; d) M. A. Bañares, J. H. Cardoso, G. J. Hutchings, J. M. C. Bueno, J. L. Fierro, *Catal. Lett.* **1998**, *56*, 149-153.

[15] N. W. Assaf, M. De La Pierre, M. K. Altarawneh, M. W. Radny, Z.-T. Jiang, B. Z. Dlugogorski, *J. Phys. Chem. C* **2017**, *121*, 11346-11354.

[16] a) X. Rozanska, R. Fortrie, J. Sauer, *J. Am. Chem. Soc.* **2014**, 136, 7751 – 7761; b) E. C. Tyo, C. Yin, M. Di Vece, Q. Qian, G. Kwon, S. Lee, B. Lee, J. E. DeBartolo, S. Seifert, R. E. Winans, R. Si, B. Ricks, S. Goergen, M. Rutter, B. Zugic, M. Flytzani-Stephanopoulos, Z. W. Wang, R. E. Palmer, M. Neurock, S. Vajda, *ACS Catalysis* **2012**, 2, 2409-2423. c) J. J. Yu, Y. Xu, V. V. Guliants, *Catal. Today* **2014**, 238, 28-34.

[17] K. Kwapien, J. Paier, J. Sauer, M. Geske, U. Zavyalova, R. Horn, P. Schwach, A. Trunschke, R. Schlögl, *Angew. Chem. Int. Ed.* **2014**, *53,* 8774-8778.

Entry for the Table of Contents (Please choose one layout)

Layout 1:

Communication

Propane ODH over h-BN undergoes both surface-mediated and gas-phase radical pathways where propene is exclusively formed from surface reaction while C_1 and C_2 products are formed via both channels.

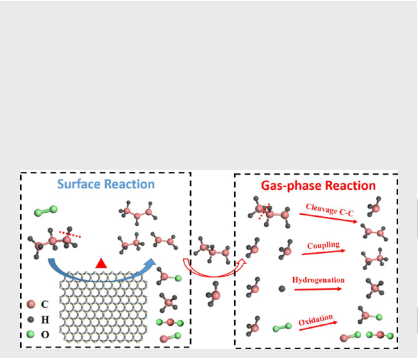

Xuanyu Zhang[+], Rui You[+], Zeyue Wei, Xiao Jiang, Jiuzhong Yang, Yang Pan, Peiwen Wu, Qingdong Jia, Zhenghong Bao, Lei Bai, Bobby Sumpter, Victor Fung, Weixin Huang* and Zili Wu**

Page No. – Page No.

Radical Chemistry and Reaction Mechanisms of Propane Oxidative Dehydrogenation over Hexagonal Boron Nitride Catalysts